Accelerated Publication

THE JOURNAL OF BIOLOGICAL CHEMISTRY
Vol. 276, No. 39, Issue of September 28, pp. 36063–36066, 2001

The gp91^{phox} Component of NADPH Oxidase Is Not the Voltage-gated Proton Channel in Phagocytes, but It Helps*

Received for publication, June 25, 2001,
and in revised form, July 24, 2001
Published, JBC Papers in Press, July 26, 2001,
DOI 10.1074/jbc.C100352200

Thomas E. DeCoursey‡§, Vladimir V. Cherny‡, Deri Morgan‡, Ben Z. Katz¶, and Mary C. Dinauer‖

From the ‡Department of Molecular Biophysics and Physiology, Rush Presbyterian St. Luke's Medical Center, Chicago, Illinois 60612, ¶Department of Pediatrics, Northwestern University Medical School, Children's Memorial Hospital, Chicago, Illinois 60614, and ‖Department of Pediatrics and Medical and Molecular Genetics, Indiana University School of Medicine, Herman B. Wells Center for Pediatric Research, Indianapolis, Indiana 46202

During the "respiratory burst," the NADPH oxidase complex of phagocytes produces reactive oxygen species that kill bacteria and other invaders (Babior, B. M. (1999) *Blood* 93, 1464–1476). Electron efflux through NADPH oxidase is electrogenic (Henderson, L. M., Chappell, J. B., and Jones, O. T. G. (1987) *Biochem. J.* 246, 325–329) and is compensated by H^+ efflux through proton channels that reportedly are contained within the gp91^{phox} subunit of NADPH oxidase. To test whether gp91^{phox} functions as a proton channel, we studied H^+ currents in granulocytes from X-linked chronic granulomatous disease patients lacking gp91^{phox} (X-CGD), the human myelocytic PLB-985 cell line, PLB-985 cells in which gp91^{phox} was knocked out by gene targeting (PLB$_{KO}$), and PLB-985 knockout cells re-transfected with gp91^{phox} (PLB$_{91}$). H^+ currents in unstimulated PLB$_{KO}$ cells had amplitude and gating kinetics similar to PLB$_{91}$ cells. Furthermore, stimulation with the phorbol ester phorbol 12-myristate 13-acetate increased H^+ currents to a similar extent in X-CGD, PLB$_{KO}$, and PLB$_{91}$ cells. Thus, gp91^{phox} is not the proton channel in unstimulated phagocytes and does not directly mediate the increase of proton conductance during the respiratory burst. Changes in H^+ channel gating kinetics during NADPH oxidase activity are likely crucial to the activation of H^+ flux during the respiratory burst.

A voltage-gated proton conductance is activated during the respiratory burst in human neutrophils (1–6). The resulting H^+ efflux compensates for the electrogenic action of NADPH oxidase (1). Several lines of evidence have suggested that the gp91^{phox} component of the NADPH oxidase complex might be the proton channel that is activated during the respiratory burst (2, 3, 7, 8). The presence of H^+ currents in monocytes from gp91^{phox}–deficient CGD[1] patients appeared to refute this idea (9), but Henderson and Chappell (10) argued that these data were inconclusive. Furthermore, it has been reported that heterologous expression of gp91^{phox} results in the appearance of proton fluxes or proton currents resembling those activated during the respiratory burst (8, 11–15). The expression systems employed to date provide ambiguous results, because CHO and HEK-293 cells express endogenous voltage-gated proton channels (14–17) and mRNA for gp91^{phox}, and four gp91^{phox} homologs have been detected by reverse transcriptase polymerase chain reaction in HEK-293 cells (18). An increase in H^+ currents after transfection might reflect expression of channels formed by the transfected gene product but could simply reflect up-regulation of constitutively expressed H^+ channels. It is also possible that expression of gp91^{phox} in a background lacking p22^{phox} might induce non-physiological behavior that is not exhibited in phagocytes. The stability of gp91^{phox} and p22^{phox} expression in phagocytes is enhanced by the formation of heterodimers of these two components of flavocytochrome b_{558} (19, 20). We therefore studied stable PLB-985 cell lines with gp91^{phox} genetically knocked-out and with gp91^{phox} re-expressed in the same background (21).

EXPERIMENTAL PROCEDURES

Cells—The PLB-985-derived cell lines were developed by Dinauer and colleagues (21). Wild-type PLB-985 cells (PLB$_{WT}$), PLB$_{KO}$ (PLB-985 cells targeted with a construct that prevents gp91^{phox} expression), and PLB$_{91}$ (gp91^{phox} knockout cells after rescue by stable transfection with gp91^{phox} cDNA) were all induced by incubation with 0.5% *N*,*N*-dimethylformamide (DMF; Sigma) for 4–7 days. Some whole-cell studies were done on PLB$_{KO}$ cells before DMF induction, designated PLB$_{KO*}$. The absence of gp91^{phox} expression in the PLB$_{KO}$ granulocytes is well documented (20–23). X-CGD granulocytes (mainly neutrophils) were isolated by density gradient centrifugation as described (24) from three patients with CGD, all of whom had documented absent neutrophil superoxide production and mutations that would prevent stable expression of gp91^{phox} (25). The specific mutations were (*a*) Cys^{1347} → Ala in Exon 11, changing the codon for Cys^{445} to a premature STOP codon; (*b*) deletion of Cys^{1028} in Exon 9, leading to a frameshift after Pro^{339} and a premature STOP three codons downstream; and (*c*) insertion of Cys after Gly^{169} in Exon 3, leading to a frameshift after Leu^{52} and a premature STOP codon in Exon 5. In patient *c*, the absence of cytochrome b_{558} was demonstrated spectrophotometrically in neutrophil extracts. Blood from patient *c* was refrigerated overnight before use, and most surviving granulocytes were identified as eosinophils in a Wright-stained cytospin preparation.

Electrophysiology—Whole-cell and permeabilized patch voltage-clamp recordings were done as described (26, 27) with micropipettes pulled from 7052 glass (Garner Glass). Whole-cell solutions (pipette and bath) included 100 mM buffer near its pK_a with tetramethylammonium$^+$ and methanesulfonate$^-$ as the main ions, 1 mM EGTA, and 1–2 mM

* This work was supported in part by the NHLBI, National Institutes of Health (to T. E. D. and M. C. D.). The costs of publication of this article were defrayed in part by the payment of page charges. This article must therefore be hereby marked "*advertisement*" in accordance with 18 U.S.C. Section 1734 solely to indicate this fact.

§ To whom correspondence should be addressed: Dept. of Molecular Biophysics and Physiology, Rush Presbyterian St. Luke's Medical Center, 1750 W. Harrison St., Chicago, IL 60612-3824. Tel.: 312-942-3267; Fax: 312-942-8711; E-mail: tdecours@rush.edu.

[1] The abbreviations used are: CGD, chronic granulomatous disease; DMF, *N*,*N*-dimethylformamide; g_H, proton conductance; I_H, H^+ current amplitude; pH_i, intracellular pH; pH_o, extracellular pH; PLB$_{KO}$, PLB-985 cells with gp91^{phox} knocked out by gene targeting; PLB$_{KO*}$, PLB-985 knockout cells before induction with DMF; PLB$_{91}$, PLB-985 knockout cells with gp91^{phox} restored; PMA, phorbol 12-myristate 13-acetate; τ_{act}, time constant of H^+ current activation; τ_{tail}, time constant of H^+ channel closing (tail current decay); $V_{threshold}$, the threshold for activating H^+ currents; X-CGD, X-linked chronic granulomatous disease; CHO, Chinese hamster ovary; HEK, human embryonic kidney; PLB$_{WT}$, wild-type PLB-985 cells; BES, 2-[bis(2-hydroxyethyl)amino]ethanesulfonic acid.

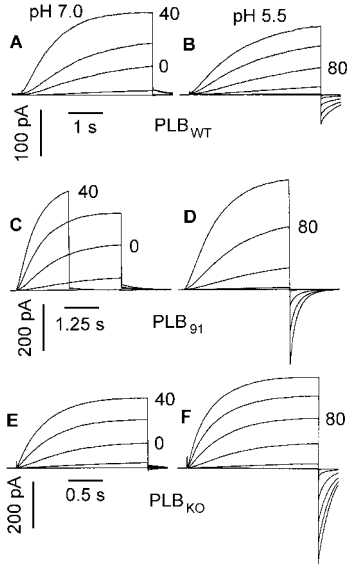

FIG. 1. **Whole-cell proton currents do not require gp91^{phox}.** Families of currents in PLB$_{WT}$ (*A* and *B*), PLB$_{91}$ (*C* and *D*), and PLB$_{KO*}$ cells (*E* and *F*) in whole-cell configuration at pH$_o$ 7.0 (*A*, *C*, and *E*) and pH$_o$ 5.5 (*B*, *D*, and *F*), all with pipette pH 5.5. Currents are in 20-mV increments, from a holding potential of −60 mV (*A*, *C*, *E*, and *F*), −40 mV (*D*), or −20 mV (*B*). The capacities were 6, 5, and 8.1 picofarad, respectively. Pulse duration was adjusted to minimize pH$_i$ depletion due to H^+ efflux.

$CaCl_2$ or $MgCl_2$. For permeabilized patch recording, all solutions contained 50 mM NH_4^+, 2 mM $MgCl_2$, 5 mM BES, 1 mM EGTA, titrated to pH 7.0 with tetramethylammonium hydroxide. The symmetrical NH_4^+ clamped pH$_i$ near 7.0 (27). Currents are shown without correction for leak or liquid junction potentials. Data were collected at 20–21 °C or at room temperature.

RESULTS

PLB$_{KO}$ Cells, Which Lack the gp91^{phox} Protein (21, 22), Express Large Voltage-gated Proton Currents—PLB-985 cells induced by DMF to granulocytic differentiation express all NADPH oxidase components and are capable of a respiratory burst (21). PLB$_{WT}$ cells had large voltage-gated proton currents (Fig. 1, *A* and *B*) that resemble those in other phagocytes and related cells (17). Proton currents in DMF-induced PLB$_{91}$ cells (Fig. 1, *C* and *D*) were similar to those in DMF-induced PLB$_{WT}$ cells, as expected. PLB$_{KO}$ cells, which do not express gp91^{phox} protein (21, 22), also had large H^+ currents both before (Fig. 1, *E* and *F*) and after induction with DMF. These results demonstrate unequivocally that gp91^{phox} is not the voltage-gated proton channel in unstimulated phagocytes.

The Selectivity and Gating Kinetics of Voltage-gated Proton Channels Are Identical Regardless of Whether gp91^{phox} Is Present—To explore whether expression of gp91^{phox} might alter the properties of H^+ channels, we characterized the H^+ currents thoroughly. Tail currents reversed near the Nernst potential for H^+ in the three PLB lines (Fig. 2*A*), confirming that protons carry these currents. The slope of the data is 51.8 mV/unit pH, which is close to the 58.2 mV given by the Nernst equation. The largest deviation from the Nernst prediction indicates that H^+ is $>10^6$ more permeant than tetramethylammonium$^+$, the main cation present. Like other H^+ channels (17), those in PLB cells are essentially perfectly H^+–selective.

The voltage dependence of H^+ current activation was very similar in PLB$_{WT}$, PLB$_{91}$, and PLB$_{KO}$ cells, as evident in average H^+ chord-conductance voltage (g_H-V) data (Fig. 2*B*). H^+ currents in PLB knockout cells studied before (PLB$_{KO}$) and after induction with DMF (PLB$_{KO*}$) were identical. The effects of changing pH$_o$ from 7.0 (Fig. 1, *A*, *C*, and *E*) to 5.5 (Fig. 1, *B*, *D*, and *F*) were similar in all cell types and to effects reported previously (17, 28).

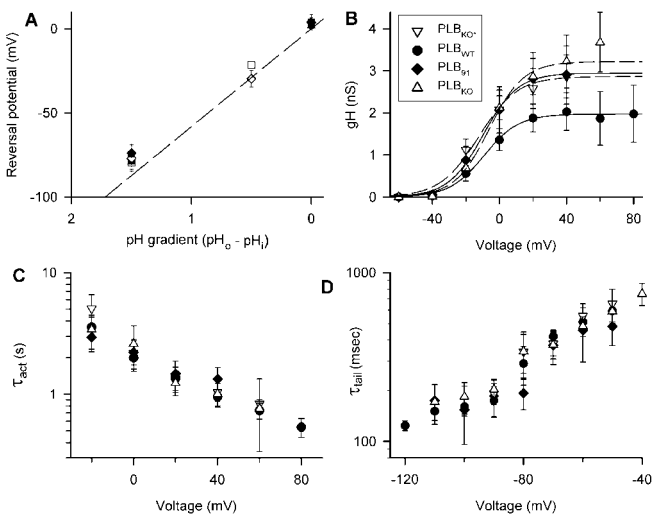

FIG. 2. **The properties of whole-cell voltage-gated proton currents are identical in PLB$_{WT}$, PLB^{KO}, and PLB^{91} cells.** ***A*,** Mean tail current reversal potentials (± S.D.; n = 2–9, total 44 measurements) are plotted for PLB$_{WT}$ (▲), PLB$_{91}$ (□, ■), and PLB$_{KO}$ (◇, ◆), where *solid symbols* indicate pH$_i$ 5.5, and *open symbols* indicate pH$_i$ 6.5. The *dashed line* is the Nernst potential for H^+. ***B*,** average g_H-V relationships for PLB$_{WT}$ (●), PLB$_{91}$ (◆), PLB$_{KO}$ (△), and PLB$_{KO*}$ (▽) cells studied at pH$_o$ 7.0 and pH$_i$ 5.5. Chord g_H was calculated by extrapolating a single exponential fit to the H^+ current and from the reversal potential measured in each solution in each cell. *Curves* show the Boltzmann curve that best fit (by non-linear least squares) each of the following sets of average g_H data: $g_H/g_{H,\,max} = [1 + \exp((V - V_{½})/k)]^{-1}$, with fitted parameters $g_{H,\,max}$ 1.97, 2.94, 3.22, and 2.86 nano Siemens; $V_{½}$ −9.2, −9.8, −6.2, and −12.4 mV; and k −10.3, −10.4, −10.3, and −11.5 mV for PLB$_{WT}$, PLB$_{91}$, PLB$_{KO}$, and PLB$_{KO*}$, respectively. ***C***, average τ_{act} measured at pH$_o$ 7.0 and pH$_i$ 5.5 (*symbols* defined in *B*). The average slope is 54 mV/*e*-fold change in τ_{act}. ***D***, average τ_{tail} from single exponential fits measured at pH$_o$ 7.0 and pH$_i$ 5.5 (*symbols* defined in *B*). The average slope is 41 mV/*e*-fold change in τ_{tail}. Data are from four to six cells for each set in *B–D*.

The behavior of the g_H in cells studied at pH$_i$ 6.5 (*not shown*) was also similar in PLB$_{91}$ and PLB$_{KO}$ cells and to that described previously (17, 28). Fig. 2, *C* and *D* shows that the kinetics of H^+ channel opening (τ_{act}) and closing (τ_{tail}), respectively, were indistinguishable in PLB-985 cells expressing (PLB$_{WT}$ and PLB$_{91}$) or lacking gp91^{phox} (PLB$_{KO}$ and PLB$_{KO*}$). Thus, the physiological properties of H^+ channels in unstimulated phagocytes are not altered by gp91^{phox} expression.

Activation of NADPH Oxidase by PMA Can Be Detected as an Electron Current in PLB$_{91}$ Cells Studied in Permeabilized Patch Configuration—The response of individual PLB$_{91}$ cells to PMA was variable, possibly reflecting variable levels of induction by DMF. We observed DPI-sensitive electron currents, which reflect NADPH oxidase activity (24, 27, 29–31), at the holding potential in about half (9 of 17) of PLB$_{91}$ cells stimulated with PMA. Electron currents usually appeared after a delay (up to 10 min) and in conjunction with a slowing of tail current decay. The average peak electron current was −2.4 ± 1.8 pA (mean ± S.D.; n = 9), similar to −2.3 pA in human neutrophils (27). This similarity is consistent with the similar levels of superoxide anion production in PMA-stimulated PLB-985 cells and human neutrophils (21).

H^+ Currents in PLB$_{91}$ Cells Studied in Permeabilized Patch Configuration Are Enhanced by PMA—The demonstration that gp91^{phox} is not the voltage-gated proton channel in unstimulated PLB-985 cells is compatible with a recent suggestion that two types of H^+ channels exist in phagocytes and that gp91^{phox} functions as a proton channel only when NADPH oxidase is active (29). In human neutrophils or eosinophils studied in permeabilized patch configuration, both NADPH oxidase and H^+ channels can be activated by PMA or arachidonic acid (24,

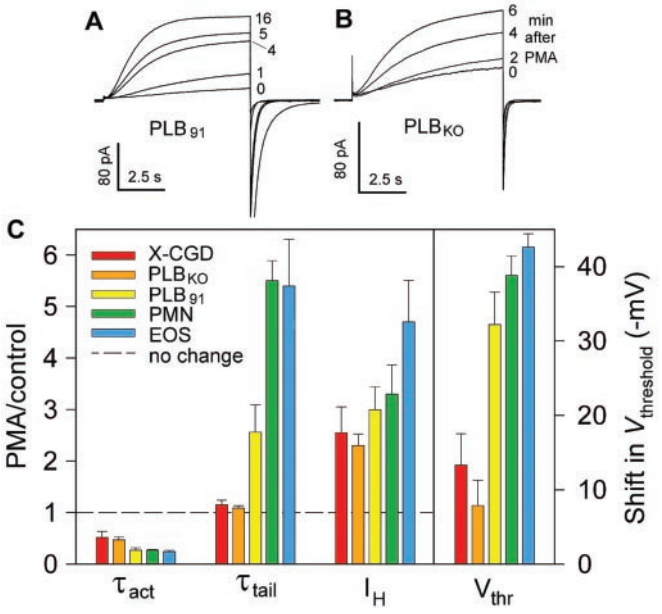

FIG. 3. **Effects of PMA stimulation on cells studied in permeabilized patch configuration.** PMA effects on a PLB_{91} cell (*A*) and a PLB_{KO} cell (*B*). Test pulses to +60 mV were applied before and after application of 60 nM PMA (*currents* labeled with the time after treatment). Note the slowing of tail current decay in *A* but not in *B*. The response of the cell in *A* was larger than typical but was selected to illustrate the changes in gating kinetics observed. *C*, average changes in H^+ current kinetics (τ_{act} and τ_{tail}), amplitude (I_H), and threshold voltage (V_{thr}; *right axis*) after PMA stimulation, compared with previously published data from human neutrophils (27) (*PMN*) and human eosinophils (24) (*EOS*). The mean ± S.E. ratio of the peak response, usually measured 5–10 min after PMA addition, to the control measurement is plotted. Numbers of cells are as follows: X-CGD, 6 (two from each patient); PLB_{KO}, 7; PLB_{91}, 9; PMN, 11–14; EOS, 12–14. Only PLB_{91} cells exhibiting electron currents upon stimulation with PMA are included; those without electron currents (not shown) responded identically to PLB_{KO} cells.

27, 31). The H^+ currents in these activated phagocytes closely resemble the NADPH oxidase-related variety described by Bánfi *et al*. (29). The H^+ current response of PLB_{91} cells to PMA was qualitatively like that of human neutrophils and eosinophils (24, 27). Fig. 3*A* illustrates H^+ currents during test pulses to +60 mV in a PLB_{91} cell. PMA stimulation produced four changes in H^+ currents in PLB_{91} cells that displayed electron currents as follows (Fig. 3*C*): (*a*) the H^+ current amplitude (I_H) increased; (*b*) activation of H^+ current during depolarizing pulses (τ_{act}) became faster; (*c*) deactivation of H^+ currents (τ_{tail}) became slower; and (*d*) the threshold for activating H^+ currents ($V_{threshold}$) was shifted 32 mV toward more negative voltages. Each change increases the likelihood of H^+ channel opening in intact cells.

PMA Increases H^+ Currents in PLB-985 Cells and Human Neutrophils to the Same Extent Regardless of Whether gp91^{phox} Is Present—Because the increase in I_H after PMA stimulation might reflect the appearance of a distinct type of proton channel related to gp91^{phox} (29), evaluating the PMA response of PLB_{KO} cells was of great interest (Fig. 3*B*). No electron current was detected, consistent with the absence of a complete NADPH oxidase complex. PMA stimulation increased I_H to a similar extent in PLB_{KO}, X-CGD, PLB_{91} cells, and neutrophils (Fig. 3*C*). Because I_H during a test pulse is an arbitrary measure, we also compared the maximum g_H, which increased after PMA stimulation by a factor of 2.06 ± 0.39 (mean ± S.D.; n = 7) in PLB_{KO} cells and 2.43 ± 1.37 (n = 9) in PLB_{91} cells ($p > 0.5$). In all cell types, H^+ current activation became faster. In parallel, we studied granulocytes from three CGD patients with mutations that prevent expression of gp91^{phox} (X-CGD). The X-CGD cells had normal or larger than normal H^+ currents, and their response to PMA was similar to that of PLB_{KO} cells. Although the mean change in τ_{act} was larger in PLB_{91} than PLB_{KO} or X-CGD cells, our exclusion from analysis of PLB_{91} cells without electron currents may account for this difference, because this criterion could not be used to exclude non-responding PLB_{KO} or X-CGD cells. The PMA-induced changes in H^+ currents in the eight PLB_{91} cells with no detectable electron currents (not shown) were identical to those in PLB_{KO} cells. Because I_H increased to a similar extent in PLB_{KO}, X-CGD, PLB_{91} cells, and human neutrophils, the increased g_H during the respiratory burst (1, 2, 4, 5) is not because of the appearance of proton currents conducted through the gp91^{phox} molecule.

PMA Elicits Fewer Changes in Gating Kinetics of Proton Channels in gp91^{phox}-deficient Cells—Although I_H increased to the same extent after PMA stimulation, the response of H^+ currents to PMA was different in cells expressing or lacking gp91^{phox}. The slowing of τ_{tail} and large hyperpolarizing shift of $V_{threshold}$ were not observed in PLB_{KO} or X-CGD cells (Fig. 3*C*). The slowing of τ_{tail} was less pronounced in PLB_{91} cells than in neutrophils and eosinophils. In most cells there was a distinct but relatively subtle slowing. The hyperpolarizing voltage shift was almost as large in PLB_{91} cells (−32 mV) as in neutrophils (−39 mV) and in eosinophils (−43 mV) stimulated with PMA under similar conditions (24, 27). This voltage shift was sufficient to result in the appearance of inward H^+ currents in some cells, a hallmark property of the NADPH oxidase-related H^+ channel (29).

DISCUSSION

The presence of robust H^+ currents in PLB_{KO} cells demonstrates unequivocally that the voltage-gated proton channel in unstimulated phagocytes is not gp91^{phox} nor does it require gp91^{phox} expression. Similarly, granulocytes (this study) or monocytes (9) from CGD patients lacking gp91^{phox} exhibit normal levels of H^+ currents. Furthermore, genetic knockout of gp91^{phox} did not detectably alter the amplitude or behavior of whole-cell H^+ currents. Voltage-gated proton channels in whole-cell studies of unstimulated phagocytes function independently of gp91^{phox}.

Bánfi *et al*. (29) proposed that there were two types of H^+ channels in eosinophils, one in resting cells and a novel variety that is observed only under conditions that permit NADPH oxidase function. This novel channel reportedly differs from that in resting cells in (*a*) activating at more negative voltages, (*b*) activating more rapidly, (*c*) deactivating more slowly, and (*d*) being more sensitive to inhibition by Zn^{2+}. We observed novel H^+ channel gating behavior during NADPH oxidase function in human neutrophils and eosinophils stimulated with PMA or arachidonic acid in permeabilized patch studies (24, 27, 31). However, we saw no evidence of multiple kinetic components in stimulated phagocytes, no correlation between the amplitude of the NADPH oxidase-generated electron currents and the amplitude of PMA-activated H^+ currents (27), and identical Zn^{2+} sensitivity of H^+ currents in resting and activated cells displaying both types of channel behavior (24). We conclude that there is one type of H^+ channel in phagocytes, whose properties are greatly altered during the respiratory burst.

Here we examined whether the increased H^+ conductance in stimulated cells is because of the appearance of additional channels formed by gp91^{phox}. PMA stimulation clearly increased I_H in cells that lack gp91^{phox} (PLB_{KO} and X-CGD). This increase was not statistically different from that in cells expressing gp91^{phox} (PLB_{91} and neutrophils). If a small gp91^{phox}–mediated H^+ conductance were also activated in neutrophils

and PLB_{91} cells, it could be only a small fraction of the total g_H. It is conceivable that under some conditions, such as heterologous expression in non-phagocytes, gp91^{phox} might function as a proton channel, but the evidence presented here indicates that it does not contribute significantly to the total proton conductance of phagocytes.

In CHO cells transfected with gp91^{phox}, arachidonic acid stimulated larger proton fluxes than in control cells (8, 11, 12). Although suggestive of enhanced H^+ channel activity, these measurements are indirect. It is difficult to determine which part of these H^+ fluxes was mediated by H^+ channels, because suppression of flux by the H^+ channel inhibitor Zn^{2+} was not demonstrated. Patch-clamp studies of CHO cells transfected with gp91^{phox} (13) reveal a large conductance with properties fundamentally different from H^+ channels in native cells. A quintessential feature of H^+ channels is potent inhibition by Zn^{2+}, which slows τ_{act} (17, 26). The conductance in CHO cells was weakly inhibited by Zn^{2+}, and no slowing of activation was evident at 200 μM Zn^{2+} (13), whereas even 1 μM Zn^{2+} slows τ_{act} 3–10-fold in cells expressing voltage-gated proton channels (24, 26). In all cells with H^+ channels, increasing pH_i shifts the voltage-activation curve by ~40 mV/unit pH (16, 17, 28). In contrast, the conductance in CHO cells was activated at −20 mV at pH_i 6.9, but no H^+ current was seen at pH_i 7.5 at voltages up to +140 mV (13). The failure to see H^+ current at pH_i 7.5 is especially surprising, because the currents at pH_i 6.9 are an order of magnitude greater than in any mammalian cell. Finally, the outward currents in CHO cells activate anomalously rapidly, within <100 ms, whereas τ_{act} for phagocyte H^+ channels is typically seconds (9, 17, 24, 27, 29, 31). It was reported recently that transient gp91^{phox} expression in COS-7 cells results in voltage-gated proton currents (15). However, the currents shown appear to reverse roughly near 0 mV at pH_o 7.5 and pH_i 5.7, where the Nernst potential for H^+ is −105 mV; thus, this conductance is not H^+–selective. Evidently, expression of gp91^{phox} in alien cell lines can induce novel conductances that differ markedly from H^+ currents in resting or activated phagocytes or any cell studied to date.

The gating kinetics of H^+ channels responded differently to PMA in cells lacking gp91^{phox}. Although it is possible that gp91^{phox} itself modulates H^+ channels, we propose that these modulations of H^+ channel function occur only in the presence of a functioning NADPH oxidase complex. The properties that are influenced by NADPH oxidase function, slower τ_{tail} and hyperpolarization of the g_H-V relationship, promote activation of the g_H at membrane potentials that might occur in intact phagocytes. The alterations in H^+ channel gating during NADPH oxidase activity probably contribute more to activating H^+ flux during the respiratory burst than does the increase in $g_{H,\,max}$.

Acknowledgments—We thank John T. Curnutte and Julie Rae for evaluation of CGD genotypes and William M. Nauseef and Larry L. Thomas for critical discussions.

REFERENCES

1. Henderson, L. M., Chappell, J. B., and Jones, O. T. (1987) *Biochem. J.* **246,** 325–329
2. Henderson, L. M., Chappell, J. B., and Jones, O. T. (1988) *Biochem. J.* **251,** 563–567
3. Henderson, L. M., Chappell, J. B., and Jones, O. T. (1988) *Biochem. J.* **255,** 285–290
4. Nanda, A., and Grinstein, S. (1991) *Proc. Natl. Acad. Sci. U. S. A.* **88,** 10816–10820
5. Kapus, A., Szászi, K., and Ligeti, E. (1992) *Biochem. J.* **281,** 697–701
6. DeCoursey, T. E., and Cherny, V. V. (1993) *Biophys. J.* **65,** 1590–1598
7. Nanda, A., Grinstein, S., and Curnutte, J. T. (1993) *Proc. Natl. Acad. Sci. U. S. A.* **90,** 760–764
8. Henderson, L. M., Banting, G., and Chappell, J. B. (1995) *J. Biol. Chem.* **270,** 5909–5916
9. Nanda, A., Romanek, R., Curnutte, J. T., and Grinstein, S. (1994) *J. Biol. Chem.* **269,** 27280–27285
10. Henderson, L. M., and Chappell, J. B. (1996) *Biochim. Biophys. Acta* **1273,** 87–107
11. Henderson, L. M., Thomas, S., Banting, G., and Chappell, J. B. (1997) *Biochem. J.* **325,** 701–705
12. Henderson, L. M. (1998) *J. Biol. Chem.* **273,** 33216–33223
13. Henderson, L. M., and Meech, R. W. (1999) *J. Gen. Physiol.* **114,** 771–786
14. Bánfi, B., Maturana, A., Jaconi, S., Arnaudeau, S., Laforge, T., Sinha, B., Ligeti, E., Demaurex, N., and Krause, K. H. (2000) *Science* **287,** 138–142
15. Maturana, A., Arnaudeau, S., Ryser, S., Bánfi, B., Hossle, J. P., Schlegel, W., Krause, K. H., and Demaurex, N. (2001) *J. Biol. Chem.* **276,** 30277–30284
16. Cherny, V. V., Henderson, L. M., and DeCoursey, T. E. (1997) *Membr. Cell Biol.* **11,** 337–347
17. Eder, C., and DeCoursey, T. E. (2001) *Prog. Neurobiol.* **64,** 277–305
18. Cheng, G., Cao, Z., Xu, X., Meir, E. G., and Lambeth, J. D. (2001) *Gene* **269,** 131–140
19. Yu, L., Zhen, L., and Dinauer, M. C. (1997) *J. Biol. Chem.* **272,** 27288–27294
20. DeLeo, F. R., Burritt, J. B., Yu, L., Jesaitis, A. J., Dinauer, M. C., and Nauseef, W. M. (2000) *J. Biol. Chem.* **275,** 13986–13993
21. Zhen, L., King, A. A., Xiao, Y., Chanock, S. J., Orkin, S. H., and Dinauer, M. C. (1993) *Proc. Natl. Acad. Sci. U. S. A.* **90,** 9832–9836
22. Biberstine-Kinkade, K. J., DeLeo, F. R., Epstein, R. I., LeRoy, B. A., Nauseef, W. M., and Dinauer, M. C. (2001) *J. Biol. Chem.* **276,** 31105–31112
23. Biberstine-Kinkade, K. J., Yu, L., and Dinauer, M. C. (1999) *J. Biol. Chem.* **274,** 10451–10457
24. DeCoursey, T. E., Cherny, V. V., DeCoursey, A. G., Xu, W., and Thomas, L. L. (2001) *J. Physiol.* **535,** 767–781
25. Heyworth, P. G., Curnutte, J. T., Rae, J., Noack, D., Roos, D., van Koppen, E., and Cross, A. R. (2001) *Blood Cells Mol. Dis.* **27,** 16–26
26. Cherny, V. V., and DeCoursey, T. E. (1999) *J. Gen. Physiol.* **114,** 819–838
27. DeCoursey, T. E., Cherny, V. V., Zhou, W., and Thomas, L. L. (2000) *Proc. Natl. Acad. Sci. U. S. A.* **97,** 6885–6889
28. Cherny, V. V., Markin, V. S., and DeCoursey, T. E. (1995) *J. Gen. Physiol.* **105,** 861–896
29. Bánfi, B., Schrenzel, J., Nüsse, O., Lew, D. P., Ligeti, E., Krause, K. H., and Demaurex, N. (1999) *J. Exp. Med.* **190,** 183–194
30. Schrenzel, J., Serrander, L., Bánfi, B., Nüsse, O., Fouyouzi, R., Lew, D. P., Demaurex, N., and Krause, K. H. (1998) *Nature* **392,** 734–737
31. Cherny, V. V., Henderson, L. M., Xu, W., Thomas, L. L., and DeCoursey, T. E. (2001) *J. Physiol.* **535,** 783–794